Journal of Colloid and Interface Science 415 (2014) 169–178

Contents lists available at ScienceDirect

Journal of Colloid and Interface Science

www.elsevier.com/locate/jcis

Metal adsorption on mosses: Toward a universal adsorption model ☆

A.G. González [a,*], O.S. Pokrovsky [a,b,*]

[a] Geosciences Environment Toulouse (GET), CNRS, UMR 5563, Observatoire Midi-Pyrénées, 14 Avenue Edouard Belin, 31400 Toulouse, France
[b] Institute of Ecological Problems of the Northern Regions, URoRAS, 23 Naberezhnaja Sev. Dviny, Arkhangelsk, Russia

ARTICLE INFO

Article history:
Received 21 July 2013
Accepted 16 October 2013
Available online 28 October 2013

Keywords:
Adsorption
Metal
Moss
pH-edge
Langmuirian isotherm

ABSTRACT

This study quantifies the adsorption of heavy metals on 4 typical moss species used for environmental monitoring in the moss bag technique. The adsorption of Cu^{2+}, Cd^{2+}, Ni^{2+}, Pb^{2+} and Zn^{2+} onto *Hypnum* sp., *Sphagnum* sp., *Pseudoscleropodium purum* and *Brachytecium rutabulum* has been investigated using a batch reactor in a wide range of pH (1.3–11.0) and metal concentrations in solution (1.6 μM–3.8 mM). A Linear Programming Model (LPM) was applied for the experimental data to derive equilibrium constants and the number of surface binding sites. The surface acid–base titration performed for 4 mosses at a pH range of 3–10 in 0.1 M $NaNO_3$ demonstrated that *Sphagnum* sp. is the most efficient adsorbent as it has the maximal number of proton-binding sites on the surface (0.65 mmol g^{-1}). The pK_a computed for all the moss species suggested the presence of 5 major functional groups: phosphodiester, carboxyl, phosphoryl, amine and polyphenols. The results of pH-edge experiments demonstrated that *B. rutabulum* exhibits the highest percentage of metal adsorption and has the highest number of available sites for most of the metals studied. However, according to the results of the constant pH "Langmuirian" isotherm, *Sphagnum* sp. can be considered as the strongest adsorbent, although the relative difference from other mosses is within 20%. The LPM was found to satisfactorily fit the experimental data in the full range of the studied solution parameters. The results of this study demonstrate a rather similar pattern of five metal adsorptions on mosses, both as a function of pH and as a metal concentration, which is further corroborated by similar values of adsorption constants. Therefore, despite the species and geographic differences between the mosses, a universal adsorption edge and constant pH adsorption isotherm can be recommended for 4 studied mosses. The quantitative comparison of metal adsorption with other common natural organic and inorganic materials demonstrates that mosses are among the most efficient natural adsorbents of heavy metals.

1. Introduction

Atmospheric pollution constitutes one of the most important environmental problems of human health [1–3]. This is especially true for heavy metal pollutions that enter the food chain via plant uptake and subsequent amplification [4]. To assess the degree of atmospheric contamination by metals, bioindicators have been widely used in both urban and industrial areas. Among various bioindicators, mosses were among the first ones for tracing pollution in Europe [5,6], notably in the industrial areas [7–13]. Their capacity to reflect the chemical composition of the surrounding atmosphere is due to the fact that mosses do not have either cuticle or root and owing to their ectohydric nature, they obtain most elements and nutrients directly from atmospheric deposition [14]. There are several other sorbents that have been tested as pollution monitors but the cost of moss production is low and they have the possibility of reutilization which, together with their high adsorption capacity, gives the moss an extra value [15]. Despite several studies on heavy metal adsorption on mosses [16,17], the detailed physico-chemical mechanism of these important biosorbents operations remains rather limited in contrast to comprehensive models and experimental data on other organic surfaces such as bacteria [18,19], fungi [20], diatoms [21,22] and organic-rich soils [23].

Moss is a phylum of small, soft plants with around 12000 species classified as Bryophyta [24] which inhabit most of the earth. Mosses are unique in the sense that they (1) are able to store water up to 16–26 times dry weight and (2) the phenolic compounds embedded in the mosses' cell walls readily avoid moss decay [25]. Peat moss can also acidify its surroundings by taking up cations such as Ca^{2+} and Mg^{2+}, and releasing H^+. These characteristics determine the very important role of moss as the interface be-

* Corresponding authors. Address: Geosciences Environment Toulouse (GET), CNRS, UMR 5563, Observatoire Midi-Pyrénées, 14 Avenue Edouard Belin, 31400 Toulouse, France. Fax: +33 561 332 650 (O.S. Pokrovsky).

E-mail addresses: aridaneglez@gmail.com (A.G. González), oleg@get.obs-mip.fr (O.S. Pokrovsky).

0021-9797/$ - see front matter © 2013 The Authors. Published by Elsevier Inc. All rights reserved.
http://dx.doi.org/10.1016/j.jcis.2013.10.028

tween atmosphere and hydrosphere/biosphere in metal biogeochemical cycles.

This work presents a concerted study of chemical characterization of four species of common European mosses, *Hypnum* sp., *Sphagnum* sp., *Pseudoscleropodium purum* and *Brachytecium rutabulum*, comprising acid–base characterization of the moss surfaces and adsorption of five toxic metals (Cu^{2+}, Cd^{2+}, Ni^{2+}, Pb^{2+} and Zn^{2+}) as a function of pH and metal concentration in solution. Nickel, cadmium and lead are especially hazardous for human health [26], causing cancer and mutations in living organisms [27–32] notably when transported as atmospheric aerosols. Copper has been responsible for neurological disorders in humans [33] and behavioral changes in animals [34]. Over the past decade, significant progress has been achieved in the application of passive biomonitors to assess the level of atmospheric contamination by heavy metals using the moss bag technique [35,36]. Despite the apparent success in using a moss bag for tracing air integral pollution [37,38], fundamental mechanisms controlling heavy metal interaction with the main sorbent, green moss, still remain poorly known and the degree of heavy metal retention by moss biomass cannot be easily predicted.

The present study is therefore aimed at quantifying the first-order physico-chemical parameters of divalent metal adsorption on moss surfaces trying to address the following specific questions:

(1) What is the most efficient metal adsorbent among 4 selected species that can be recommended for the moss bag biomonitoring procedure?
(2) What is the chemical nature of the main metal-binding group at the moss surface and how does it vary depending on moss species, the identity and aqueous concentration of metals?
(3) Can we suggest "universal" thermodynamic adsorption parameters for the prediction of metal adsorption on mosses under a wide range of solution parameters?

Via providing straightforward and quantitative answers to the above-listed questions we create a comprehensive model of chemical reactions between heavy metals and the moss-aqueous solution interface, suitable for a number of environmental applications.

2. Experimental

2.1. Moss species

The mosses examined in this research study were the dominant European species: *Hypnum* sp., *Sphagnum* sp., *P. purum* and *B. rutabulum*. They were harvested in June 2012 in NW Spain in non-urban areas. Before the experiments, the whole moss was cleaned three times with Milli-Q water (18 MQ) and inactivated at 120 °C following the standard procedure of moss bag preparation [36]. Intact whole mosses without grinding or disaggregation were used throughout the study because the physical and biological status of mosses under investigation should be as close as possible to that of moss bags envisaged in the environmental exposure conditions. The biomass concentration in the experiments was kept constant at 1 $g_{dry}\,L^{-1}$.

2.2. Chemicals

The adsorption experiments were carried out at 20 °C individually for each metal for Cu^{2+}, Cd^{2+}, Ni^{2+}, Pb^{2+} and Zn^{2+}. All metals were used as nitrate salts (Sigma–Aldrich). The electrolyte solution was 0.01 M $NaNO_3$ for all the experiments. All the solutions were prepared with Milli-Q water (18 MQ). The experiments were carried out at constant pH and were buffered by 2.5 mM MES (Merck) for pH 5.5, or HEPES for pH 6.5 (Sigma–Aldrich).

2.3. Surface acid–base titration

The acid–base titration of moss surfaces was carried out in 0.01 M $NaNO_3$ at room temperature (20 ± 1 °C). Solutions were conditioned for 1 h before titration and were also pre-saturated with nitrogen. The titration was performed in two steps, acid titration by adding aliquots of 0.07 M HCl and basic titration by adding small amounts of 0.09 M NaOH. The acid–base titration experiments were done by triplicate for each moss in a whole range of pH between 3 and 11. The reference solution was the supernatant solution after the conditioning time and removing the moss biomass. The pH was measured by a combined electrode (Mettler Toledo^{R}) in a pH-meter ion analyzer (PHM250-Meterlab™) with an uncertainty of ±0.002 units. The excess of charge was computed as the difference of the acid–base concentration in the suspension and in the reference solution according to usual procedures of biomass titration [39,40].

2.4. Adsorption of metals onto moss

The metal adsorption experiments were designed to provide a quantitative physico-chemical characterization of metal binding by moss species as a function of pH (pH-dependent adsorption edge) and as a function of aqueous metal concentration (adsorption isotherm). All the experiments were performed in the solution undersaturated with respect to any metal oxide, hydroxide or carbonate as verified by speciation calculations with the MINTEQA2 computer code and corresponding database [41,42]. Experiments were performed in polypropylene beakers continuously agitated with a suspended Teflon coated magnet stirrer and N_2 bubbling.

In the pH-edge experiments, the initial metal concentration was set at 52 μM, 29 μM, 56 μM, 16 μM and 50 μM for Cu^{2+}, Cd^{2+}, Ni^{2+}, Pb^{2+} and Zn^{2+} respectively, while the pH ranged from 1.28 to 11.02, depending on each metal. The pH was adjusted by adding aliquots of NaOH (0.1–0.01 M) or HNO_3 (0.1–0.01 M). In the second series of experiments, at constant pH (Langmuirian adsorption isotherm), the metal ion concentration ranged as follows: 1.6 μM–3.8 mM M for Cu^{2+}, 2.3 μM–1.5 mM M for Cd^{2+}, 9.1 μM–3.2 mM M for Ni^{2+}, 1.9 μM–1.0 mM M for Pb^{2+} and 7.0 μM–2.9 mM M for Zn^{2+}. In this case, the pH was kept constant by adding MES (pH ≈ 5.5) for Cu^{2+} and Pb^{2+}, or HEPES (pH ≈ 6.5) for Cd^{2+}, Ni^{2+} and Zn^{2+}.

The adsorption of Cu^{2+} and Zn^{2+} was also studied in a series of kinetics experiments conducted for *Sphagnum* sp., at constant pH and various metal concentrations in solution, via ranging the exposure time from 5 min to 28 days. These experiments demonstrated the lack of any measurable effect of the exposure time between 5 min and 28 days on the adsorbed metal concentration (see below). As such, the time of contact was 5 min for most of the adsorption experiments.

All sampled solutions were filtered (0.45 μm) and acidified with bidistilled HNO_3 and analyzed for aqueous metal concentration using flame atomic adsorption spectroscopy (Perkin Elmer AAnalyst 400) with an uncertainty of ±2% and a detection limit of 0.05 $mg\,L^{-1}$. The concentration of metal for the initial moss biomass was measured by ICP-MS (Agilent 7500 series) with a detection limit of 0.001 $\mu g\,L^{-1}$ and precision of ±5%.

The Dissolved Organic Carbon (DOC) concentration in solution was monitored for most of the experiments and was analyzed by using a Carbon Total Analyzer (Shimadzu TOC-V_{CSN}) with an uncertainty of 3% and a detection limit of 0.1 $mg\,L^{-1}$. Altogether, 170 individual experiments for 5 metals and 4 mosses were performed in this study.

2.5. Lineal Programming Model (LPM)

The LPM model was applied for the acid–base surface titration, pH-edge and fixed pH experiments in order to compute the apparent equilibrium constants and the site densities for each individual experiment following the approaches elaborated for bacteria [39,40,43]. This model is convenient for describing complex 3-D multi-layer systems having both organic components and rigid cell walls [44–46]. The details of the model description are presented in the Electronic supplementary material (ESM-1).

3. Results

In order to define the optimal experimental conditions for adsorption experiments, notably the minimal metal concentration in solution and at the moss surface, two types of preliminary experiments were conducted: (1) analysis of bulk metal concentration in non-contaminated mosses, prior to the adsorption experiments, and (2) metal release from non-contaminated mosses into aqueous solution at the typical condition of adsorption experiments.

3.1. Metal concentration in mosses

The total elementary composition of the studied mosses is listed in the Electronic supplementary material (Table ESM-1). It can be seen that Zn^{2+} was the most abundant metal for each moss (27–40 mg kg^{-1}), except for *Sphagnum* sp., where Pb^{2+} showed the highest concentration (42.9 mg kg^{-1}). According to their elementary composition, the studied mosses can be ranked in the following order: for Cu^{2+}, *B. rutabulum* > *Hypnum* sp. > *P. purum* > *Sphagnum* sp., for Cd^{2+}, *Sphagnum* sp. > *Hypnum* sp. ≈ *P. purum* ⩾ *B. rutabulum*, for Ni^{2+}, *B. rutabulum* > *Hypnum* sp. > *Sphagnum* sp. > *P. purum*, for Pb^{2+}, *Sphagnum* sp. > *Hypnum* sp. > *B. rutabulum* > *P. purum*. Finally, for Zn^{2+}, *P. purum* > *B. rutabulum* > *Sphagnum* sp. > *Hypnum* sp. Based on these results, we defined the minimal charge of moss surface by adsorbed metals as a factor of 2 higher than the metal concentration in intact biomass.

3.2. Metal release by moss

The metal released by the intact biomass into aqueous solution reflects the degree of moss degradability under given experimental conditions. The concentration of released metal therefore defined the minimal threshold of aqueous metal loading in moss adsorption experiments. Below this threshold value, specific for each metal and each moss, the addition of metal in solution for adsorption on selected biomass was considered unwarranted. For the purpose of quantifying this threshold value, the released metal concentration of Cu^{2+}, Cd^{2+}, Ni^{2+}, Pb^{2+} and Zn^{2+} was measured in 0.01 M $NaNO_3$ for a 1 g_{dry} L^{-1} biomass of each moss, after 1 min, 12 min, 1 h, 5 h and 8.5 h of exposure (Table ESM-2). Typically, the released metal concentrations are 2 orders of magnitude lower than the minimal (starting) metal concentration in our adsorption experiments. As such, the released metals do not interfere with adsorption constant measurements in this study.

According to the released metal ion concentrations, the studied moss species can be ranked as follows: for Cu^{2+} and Pb^{2+}, *B. rutabulum* > *P. purum* > *Sphagnum* sp. ⩾ *Hypnum* sp. For Cd^{2+}, *P. purum* > *B. rutabulum* > *Hypnum* sp. ⩾ *Sphagnum* sp. For Ni^{2+}, *B. rutabulum* > *Hypnum* sp. > *Sphagnum* sp. ⩾ *P. purum*. For Zn^{2+}, *P. purum* > *B. rutabulum* > *Sphagnum* sp. ≈ *Hypnum* sp.

Table ESM-2 also shows that the DOC concentration in solution and contacting with mosses increased with time during the first 1.5 h of experiments, and then stabilized around 38 mg L^{-1}, 21 mg L^{-1}, 60 mg L^{-1} and 61 mg L^{-1} for *Hypnum* sp., *Sphagnum* sp., *P. purum* and *B. rutabulum*, respectively. In this regard, *Sphagnum* sp. and *Hypnum* sp. seem to be the most inert and stable moss species in neutral aqueous solutions excreting the lowest amount of DOC.

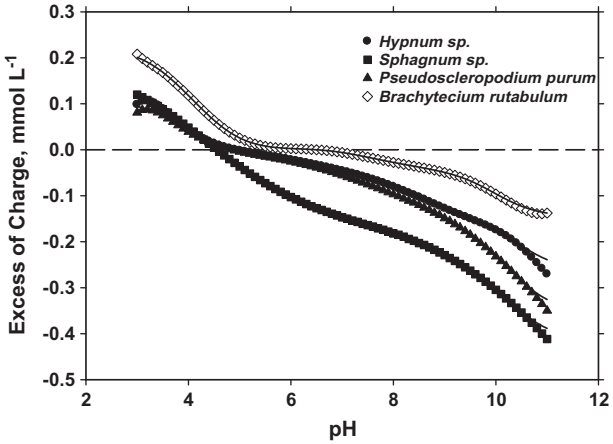

Fig. 1. Surface acid–base titration of each moss species in 0.01 M $NaNO_3$ and 1.0 g_{dry} L^{-1} biomass. Each experiment was carried out by triplicate. The solutions were conditioned during 1 h. Lines represent the LPM model results.

Table 1
Surface acid–base titration and LPM parameters for moss in 0.01 M $NaNO_3$ with 1.0 g_{dry} L^{-1} of biomass. Conditioning time of 1 h.

Species	pK_a	Binding sites mmol g^{-1}	Possible functional group
Hypnum sp. (S_T = 3)	3.70	$1.83 \cdot 10^{-1}$	Carboxyl/phosphodiester
	5.35	$1.10 \cdot 10^{-2}$	Carboxyl
	6.10	$2.13 \cdot 10^{-2}$	Phosphoryl
	6.90	$3.32 \cdot 10^{-2}$	Phosphoryl
	7.73	$3.45 \cdot 10^{-2}$	Amine
	8.68	$6.66 \cdot 10^{-2}$	Amine
	10.43	$1.40 \cdot 10^{-2}$	Polyphenol
Sphagnum sp. (S_T = 3)	3.58	$1.56 \cdot 10^{-1}$	Carboxyl/phosphodiester
	4.73	$9.48 \cdot 10^{-2}$	Carboxyl
	5.63	$4.77 \cdot 10^{-2}$	Carboxyl
	6.45	$3.43 \cdot 10^{-2}$	Phosphoryl
	7.05	$3.10 \cdot 10^{-2}$	Phosphoryl
	7.85	$3.36 \cdot 10^{-2}$	Amine
	8.05	$2.84 \cdot 10^{-2}$	Amine
	9.10	$6.72 \cdot 10^{-2}$	Amine
	10.30	$1.56 \cdot 10^{-1}$	Polyphenol
Pseudoscleropodium purum (S_T = 3)	3.75	$1.52 \cdot 10^{-1}$	Carboxyl/phosphodiester
	4.95	$1.85 \cdot 10^{-2}$	Carboxyl
	5.75	$1.70 \cdot 10^{-2}$	Carboxyl
	6.55	$2.42 \cdot 10^{-2}$	Phosphoryl
	7.30	$3.46 \cdot 10^{-2}$	Phosphoryl
	8.00	$3.40 \cdot 10^{-2}$	Amine
	9.05	$6.77 \cdot 10^{-2}$	Amine
	10.30	$2.06 \cdot 10^{-1}$	Polyphenol
Brachytecium rutabulum (S_T = 3)	3.60	$1.51 \cdot 10^{-1}$	Carboxyl/phosphodiester
	4.50	$1.22 \cdot 10^{-1}$	Carboxyl
	5.93	$1.52 \cdot 10^{-2}$	Phosphoryl
	7.35	$3.38 \cdot 10^{-2}$	Phosphoryl
	8.18	$1.21 \cdot 10^{-2}$	Amine
	9.15	$1.32 \cdot 10^{-2}$	Amine
	10.13	$1.38 \cdot 10^{-1}$	Polyphenol

3.3. Surface acid–base titration

Surface acid–base titration allows to quantify the proton and hydroxyl buffer capacity of mosses in a wide range of pH and thus determines the concentration of amphoteric surface functional

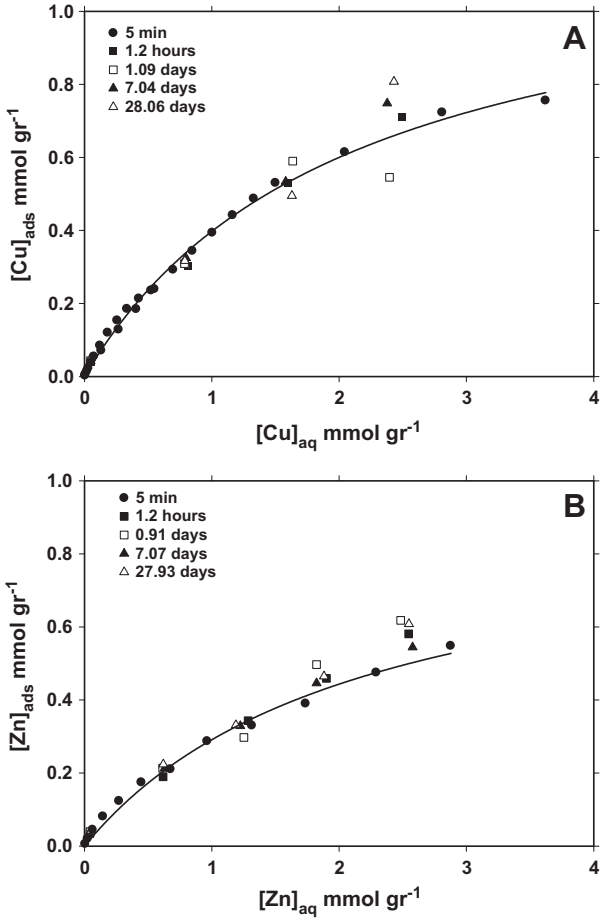

Fig. 2. Long-term adsorption of copper (A) at pH = 5.30 ± 0.01 and zinc (B) at pH = 6.20 ± 0.05. $[Cu^{2+}]$ = 0.05–2.42 mmol g^{-1} and $[Zn^{2+}]$ = 0.04–2.54 mmol g^{-1}. Biomass was always kept constant as 1.0 g_{dry} L^{-1}.

groups. These acid–base titrations were performed for a pH range from 3 to 11 as illustrated in Fig. 1. The pH values of the zero net proton adsorption (pH_{PZC}) were equal to 5.01 ± 0.13 (*Hypnum* sp.), 4.64 ± 0.10 (*Sphagnum* sp.), 4.96 ± 0.14 (*P. purum*) and 6.23 ± 0.25 (*B. rutabulum*). These differences in pH_{PZC} can be understood in terms of the different concentrations of surface functional groups of each moss species. *B. rutabulum* showed the highest excess of adsorbed protons (0.21 mmol L^{-1}), whereas *Sphagnum* sp. exhibits the highest negative surface charge. Consequently *Sphagnum* sp. may be the most efficient cation adsorbent, as it has the highest number of negatively charged moieties on the surface.

The results of the LPM application for the surface titration experiments are summarized in Table 1. The moss species can be ranked according to the total number of binding sites available on the surface as: *Sphagnum* sp. (0.65 mmol g^{-1}) > *P. purum* (0.55 mmol g^{-1}) > *Hypnum* sp. (0.49 mmol g^{-1}) ⩾ *B. rutabulum* (0.48 mmol g^{-1}). The values of pK_a obtained from the LPM fit can be tentatively linked to several possible functional groups: phosphodiester (pK_a = 3.6–3.7), carboxyl (pK_a = 4.7–5.7), phosphoryl (pK_a = 5.9–7.4), amine (pK_a = 7.7–9.2) and polyphenols (pK_a = 10.1–10.4), present in all of the four moss species.

3.4. Long-term adsorption of metals

The adsorption of Cu^{2+} and Zn^{2+} was studied as a function of the metal ion concentration in solution (0.04–2.6 mM) over different exposure periods, from 5 min to 28 days (Fig. 2). The result of these experiments allows us to choose the optimal exposure time for adsorption of metals on moss. It is shown from Fig. 2 that the adsorption of Cu^{2+} and Zn^{2+} achieved the maximum during the first 5 min. The adsorption of Cu^{2+} and Zn^{2+} was similar at different exposure times, thus strongly suggesting the achievement of an adsorption equilibrium during the first several minutes of reaction.

3.5. Adsorption of metals as a function of pH (pH-edge)

The adsorption of Cu^{2+}, Cd^{2+}, Ni^{2+}, Pb^{2+} and Zn^{2+} on moss was studied as a function of pH that ranged from 1.8 to 6.5, 1.3 to

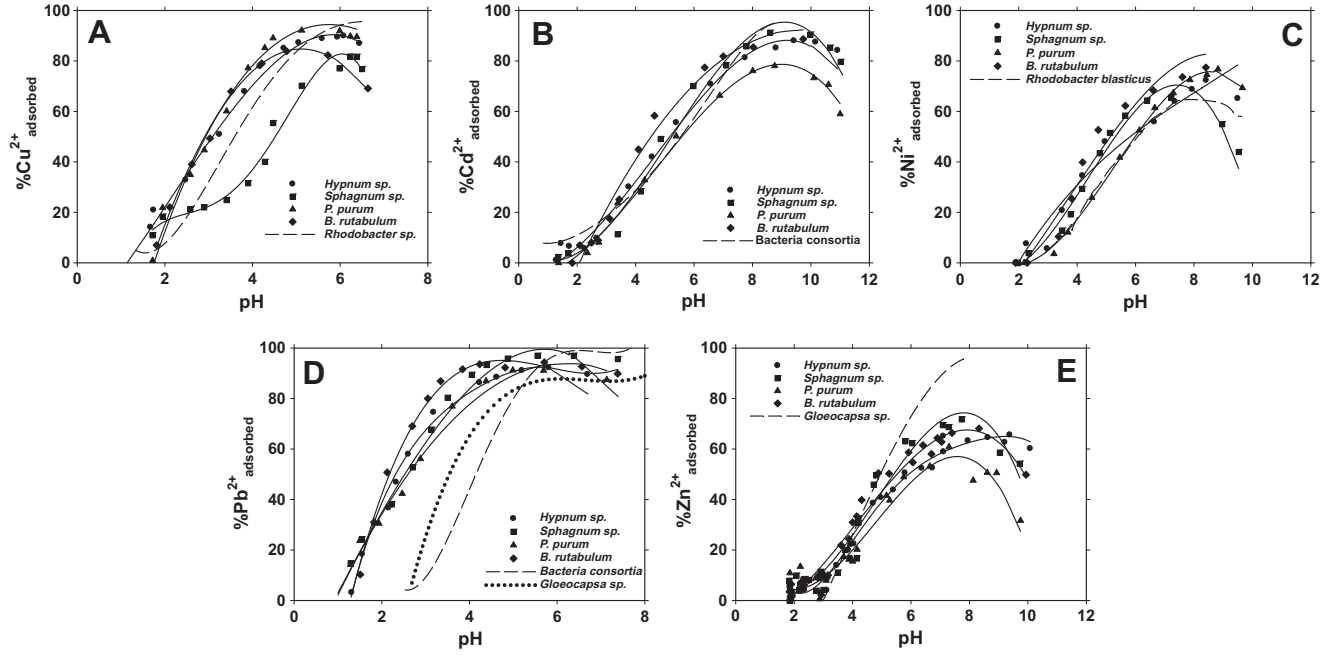

Fig. 3. Percentage of metal adsorbed onto moss surface as a function of pH, in 0.01 M $NaNO_3$ and 1.0 g_{dry} L^{-1} biomass. Initial metal concentration 0.052 mM. Lines represent the LPM model results. Dashed line was recalculated from Pokrovsky et al. [64] at 4 g_{wet} L^{-1} (A), Borrok et al. [48] at 10 g_{dry} L^{-1} (B), Pokrovsky et al. [40] at 10 g_{wet} L^{-1} (C), Ginn and Fein [83] at 1 g_{dry} L^{-1} and Pokrovsky et al. [43] at 4 g_{wet} L^{-1} (D), Pokrovsky et al. [43] (E) at 1.01 g_{dry} L^{-1}.

11.0, 1.9 to 10.5, 1.3 to 7.4, and 1.8 to 10.1, for Cu^{2+}, Cd^{2+}, Ni^{2+}, Pb^{2+} and Zn^{2+}, respectively (Fig. 3). The pH-dependent adsorption edge is rather similar among all mosses, in the first-order agreement with the principal of "universal adsorption edge" developed earlier for heterotrophic bacteria and their consortia [19,39,47,48].

The adsorption of metals typically starts at pH around 2 and the maximum adsorption percentage is achieved at pH > 6 depending on the identity of the metal. For Cu^{2+}, the adsorption was 82% at pH 6.1 for *Sphagnum* sp. whereas the highest percentage of adsorption was reached for *P. purum* (92%) at pH 5.2. For Cd^{2+}, the maximum adsorption was reached at pH 8.7 (91%) for *Sphagnum* sp. The lowest adsorption of Cd^{2+} percentage, 79%, was at pH = 8.8 for *P. purum*. For Ni^{2+}, *Sphagnum* sp. also had the highest adsorption capacity with 70% at pH = 7.2. The adsorption of Pb^{2+} was quite similar among different species (around 97% at pH = 5.5). Finally, Zn^{2+} exhibited the lowest maximal adsorption of 73% at pH = 7.8 on *Sphagnum* sp.

Based on the results of the pH-dependent adsorption edge, the mosses investigated in this study can be ranked as following: for Cu^{2+}, *P. purum* > *B. rutabulum* ⩾ *Hypnum* sp. > *Sphagnum* sp., for Cd^{2+}, *B. rutabulum* > *Sphagnum* sp. ⩾ *P. purum* > *Hypnum* sp., for Ni^{2+}, *B. rutabulum* > *P. purum* ≈ *Hypnum* sp. ≈ *Sphagnum* sp., for Pb^{2+}, *B. rutabulum* ≈ *Sphagnum* sp. ≈ *Hypnum* sp. ≈ *P. purum* and finally for Zn^{2+}, *B. rutabulum* ⩾ *Sphagnum* sp. ⩾ *Hypnum* sp. ⩾ *P. purum*.

A plot of DOC concentration as a function of pH during metal adsorption experiments demonstrated a slight increase in DOC with pH (Fig. 4). Among 4 studied mosses, *P. purum* and *B. rutabulum* are the most reactive species, excreting ⩾2 times more DOC compared to *Sphagnum* sp. and *Hypnum* sp. Therefore, *Sphagnum* sp. and *Hypnum* sp. are the most inert species in terms of biomass degradation and organic carbon leaching. This conclusion is consistent with results of metal release from the moss biomass (see Section 3.2).

The LPM model was applied for the experimental data on the pH-dependent adsorption edge of divalent metals examined in this study (Table 2). The smallest pK_s corresponding to the strongest binding were found for *Sphagnum* sp., −3.15 and −4.40 for Cu^{2+} and Cd^{2+} respectively. For Ni^{2+}, *Hypnum* sp. yielded pK_s of −3.50, and for Pb^{2+} and Zn^{2+}, *B. rutabulum* showed the strongest binding pK_s, −3.20 and −0.65, respectively. The number of surface binding sites capable of adsorbing cationic metals was computed to be the highest for *P. purum* ($4.0 \cdot 10^{-2}$ mmol g^{-1}) in the presence of Cu^{2+}. *Sphagnum* sp. contained $1.8 \cdot 10^{-2}$ mmol g^{-1} for Cd^{2+} adsorption experiments, whereas *B. rutabulum* exhibited the highest number of sites for Ni^{2+}, Pb^{2+} and Zn^{2+} with $3.2 \cdot 10^{-2}$, $1.3 \cdot 10^{-2}$ and $2.0 \cdot 10^{-2}$ mmol g^{-1}, respectively.

3.6. Adsorption of metals as a function of metal concentration in solution ("Langmuirian" isotherm)

The adsorption of Cu^{2+}, Cd^{2+}, Ni^{2+}, Pb^{2+} and Zn^{2+} on *Hypnum* sp., *Sphagnum* sp., *P. purum* and *B. rutabulum* was studied at constant pH 5.5, 6.5, 5.6, 6.5 and 6.8 respectively, in the range of

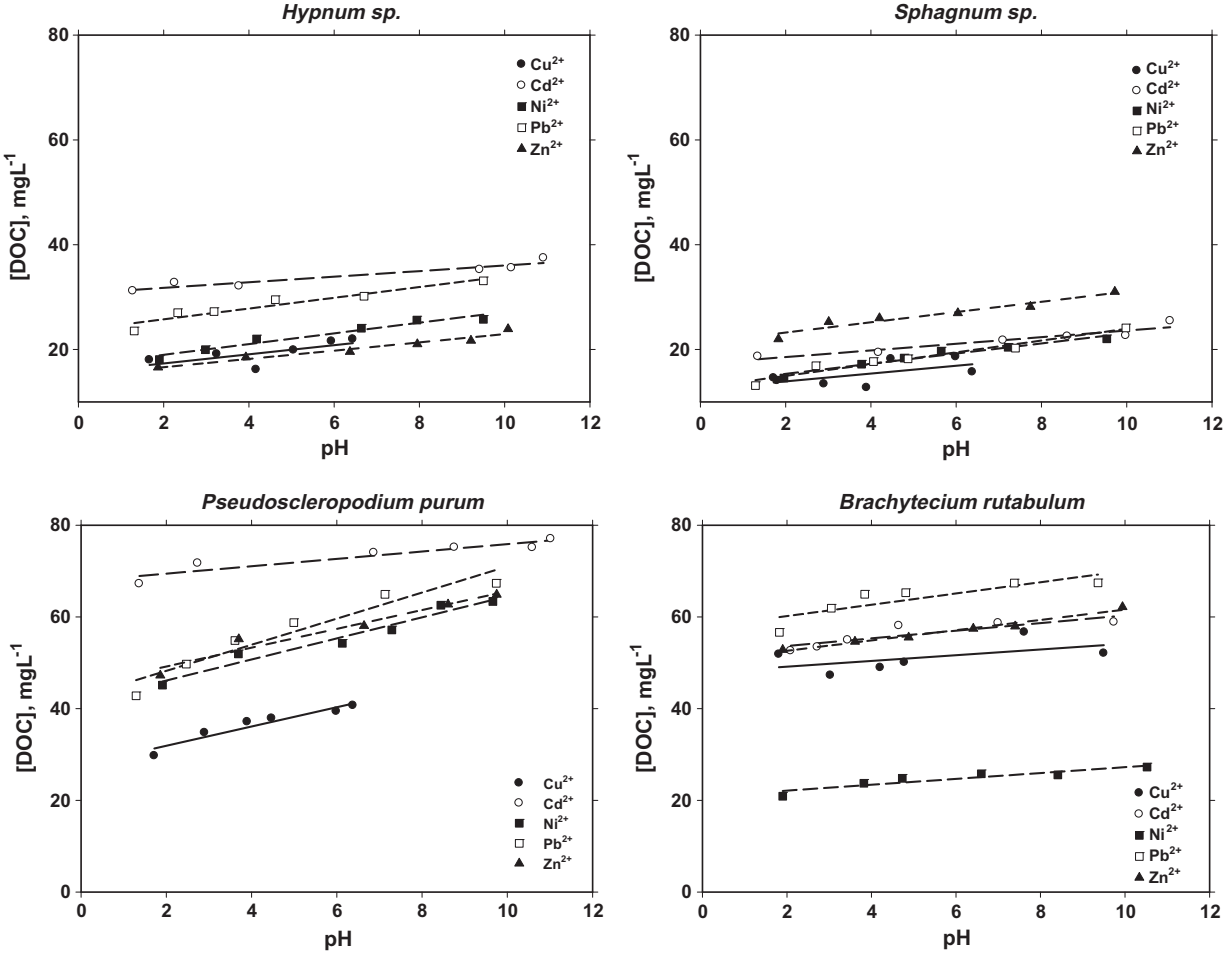

Fig. 4. Dissolved Organic Carbon measured during metal adsorption experiments as a function of pH, in 0.01 M $NaNO_3$ and 1.0 g_{dry} L^{-1} biomass.

Table 2
Experimental conditions and LPM parameters for metal adsorption on moss as a function of pH in 0.01 M $NaNO_3$ with biomass of 1.0 g_{dry} L^{-1}. K_s corresponds with the equilibrium constant for the reaction between metal in solution and the available sites as a function of pH.

Species	Metal studied	pH-range	[Me^{2+}] μM	pK_s	Binding sites mmol g^{-1}
Hypnum sp.	Copper	1.67–6.44	51.94	−1.80	$3.32 \cdot 10^{-2}$
Sphagnum sp.		1.72–6.50		−3.15	$8.69 \cdot 10^{-3}$
				−0.60	$1.95 \cdot 10^{-2}$
Pseudoscleropodium purum		1.72–6.38		−1.90	$3.96 \cdot 10^{-2}$
Brachytecium rutabulum		1.81–6.63		−2.05	$3.49 \cdot 10^{-2}$
Hypnum sp.	Cadmiun	1.28–10.21	29.36	−4.15	$1.28 \cdot 10^{-3}$
				−1.30	$8.55 \cdot 10^{-3}$
				0.25	$9.29 \cdot 10^{-3}$
Sphagnum sp.		1.35–11.02		−4.40	$8.26 \cdot 10^{-4}$
				−0.35	$1.78 \cdot 10^{-2}$
Pseudoscleropodium purum		1.37–11.02		−1.55	$7.81 \cdot 10^{-3}$
				0.00	$7.85 \cdot 10^{-3}$
Brachytecium rutabulum		1.84–9.74		−2.50	$1.31 \cdot 10^{-3}$
				−1.05	$1.38 \cdot 10^{-2}$
				−0.15	$6.97 \cdot 10^{-3}$
Hypnum sp.	Nickel	1.90–9.50	56.23	−3.50	$5.71 \cdot 10^{-4}$
				−0.70	$2.46 \cdot 10^{-2}$
Sphagnum sp.		1.96–9.53		−0.55	$2.48 \cdot 10^{-2}$
Pseudoscleropodium purum		1.91–9.66		−0.60	$6.38 \cdot 10^{-3}$
				0.15	$1.95 \cdot 10^{-2}$
Brachytecium rutabulum		1.90–10.52		−0.50	$3.20 \cdot 10^{-2}$
Hypnum sp.	Lead	1.31–6.70	15.93	−2.95	$1.27 \cdot 10^{-2}$
Sphagnum sp.		1.29–7.39		−3.00	$1.30 \cdot 10^{-2}$
Pseudoscleropodium purum		1.29–7.13		−2.95	$1.11 \cdot 10^{-2}$
Brachytecium rutabulum		1.51–7.38		−3.20	$1.32 \cdot 10^{-2}$
Hypnum sp.	Zinc	1.87–10.08	50.48	−0.55	$1.57 \cdot 10^{-2}$
Sphagnum sp.		1.83–9.72		−0.45	$1.81 \cdot 10^{-2}$
Pseudoscleropodium purum		1.86–9.75		−0.35	$1.39 \cdot 10^{-2}$
Brachytecium rutabulum		1.90–9.94		−0.65	$2.00 \cdot 10^{-2}$

1.6 μM–3.8 mM (Cu^{2+}), 2.3 μM–1.5 mM (Cd^{2+}), 9.1 μM–3.2 mM (Ni^{2+}), 1.9 μM–1.0 mM (Pb^{2+}) and 7.0 μM–2.9 mM (Zn^{2+}) as shown in Table 3 and Fig. 5. The adsorption curve is rather similar among all four mosses and depends significantly on the identity of the metal. The concentration of adsorbed metal increased linearly with $[Me^{2+}]_{aq}$ until 0.5 mM. Above this concentration, Cu^{2+}, Cd^{2+}, Ni^{2+}, and, in a lesser degree, Pb^{2+}, demonstrated the beginning of surface sites saturation.

The Langmuirian adsorption isotherm describes a large number of adsorption experiments on biosorbents [49]. It was used to rationalize the adsorption data according to the following:

$$\frac{[Me^{2+}]_{aq}}{[Me^{2+}]_{ads}} = \frac{1}{K_L q_{max}} + \frac{[Me^{2+}]_{aq}}{q_{max}} \quad (1)$$

where K_L is the Langmuir equilibrium (g $mmol^{-1}$) constant and q_{max} is the maximum adsorption capacity (mmol g^{-1}). This equation provided an adequate fit to the data with $R^2 > 0.98$; obtained Langmuirian parameters are listed in Table 4.

The highest value of K_L was obtained for Ni^{2+} adsorption (7.1–11.4 g $mmol^{-1}$) while the K_L for adsorption of Cu^{2+}, Pb^{2+} and Zn^{2+} ranged between 0.3 and 1.0 g $mmol^{-1}$. The maximum adsorption capacity (q_{max}) was reached for Pb^{2+} on *B. rutabulum* (2.6 mmol g^{-1}). An integral parameter of metal adsorption on mosses is defined as the sum of all 4 metals q_{max} value which follows the order: *B. rutabulum* (4.9 mmol g^{-1}) > *Sphagnum* sp. (4.2 mmol g^{-1}) > *Hypnum* sp. (3.6 mmol g^{-1}) > *P. purum* (3.5 mmol g^{-1}).

Individually for each metal, the moss adsorption capacity can be ranked as follows: For Cu^{2+}, *P. purum* ⩾ *Sphagnum* sp. > *Hypnum* sp. ⩾ *B. rutabulum*; for Cd^{2+}, *Sphagnum* sp. > *B. rutabulum* ⩾ *Hypnum* sp. > *P. purum*; for Ni^{2+}, *Sphagnum* sp. ⩾ *Hypnum* sp. ⩾ *B. rutabulum* ⩾ *P. purum*; for Pb^{2+}, *B. rutabulum* > *Hypnum* sp. > *Sphagnum* sp. > *P. purum*; for Zn^{2+}, *B. rutabulum* ⩾ *Sphagnum* sp. ≈ *P. purum* ⩾ *Hypnum* sp.

Overall, *Sphagnum* sp. can be considered to be among the strongest adsorbents, although the relative differences to other mosses are within 20%.

All the data collected for Langmuir isotherm experiments were used to apply the LPM model and the results are shown in Table 3. The LPM revealed small but statistically significant differences in metal binding by different species. In particular, *Hypnum* exhibited the highest amount of binding sites for Cd^{2+} (40 mmol g^{-1}), Pb^{2+} (50 mmol g^{-1}) and Ni^{2+} exposure (8 mmol g^{-1}), and *Sphagnum* sp. exhibited the maximal amount of binding sites for Zn^{2+} (29 mmol g^{-1}) among 4 moss species.

4. Discussion

4.1. Moss chemical composition and degradation in aqueous solution

The total chemical composition of the four moss species examined in this research study is in general agreement with results reported for other moss species [50–52]. In particular, Castello [52] reported the chemical composition of *H. cupressiforme* and *P. purum*. while for both *P. purum* the concentration of Al, Cu and Zn is in the same order; As, Cd, Cr, Fe, and Pb concentrations are lower in the present study and Mn and Ti concentrations are higher in this study compared to Castello [52]. Overall, all studied species are enriched in Al, As, Fe, Mn, and Ti and *Sphagnum* sp. and *B. rutabulum* are enriched in Pb and Cr, respectively, compared to the literature data.

The differences in composition between mosses could be understood in terms of morphologic specificity and growth rates. The smaller species are able to form compact communities and more crowded leaves allow them to reach high efficiency to bind metals [50]. In terms of growth rate, the species with lower rates

Table 3
Experimental conditions and LPM parameters for metal adsorption on moss as a function of metal concentration in solution (Langmurian-isotherm) in 0.01 M $NaNO_3$ with biomass of 1.0 g_{dry} L^{-1}. K_m corresponds with the equilibrium constant for the reaction between metal in solution and the available sites as a function metal aqueous concentration in solution.

Species	Metal studied	pH-range	[Me^{2+}] M	pK_m	Binding sites mmol g^{-1}
Hypnum sp.	Copper	5.50 ± 0.04	$5.19 \cdot 10^{-6}$–$3.65 \cdot 10^{-3}$	2.25	0.430
				5.10	34.828
Sphagnum sp.		5.52 ± 0.03	$1.57 \cdot 10^{-6}$–$3.62 \cdot 10^{-3}$	0.70	0.051
				2.65	1.038
Pseudoscleropodium purum		5.51 ± 0.04	$1.57 \cdot 10^{-6}$–$3.78 \cdot 10^{-3}$	0.75	0.104
				2.85	1.220
Brachytecium rutabulum		5.53 ± 0.04	$9.13 \cdot 10^{-6}$–$2.85 \cdot 10^{-3}$	1.45	0.181
				2.40	0.523
Hypnum sp.	Cadmiun	6.52 ± 0.04	$2.31 \cdot 10^{-6}$–$1.41 \cdot 10^{-3}$	2.55	0.172
				5.90	14.526
Sphagnum sp.		6.52 ± 0.05	$2.31 \cdot 10^{-6}$–$1.34 \cdot 10^{-3}$	1.45	0.029
				3.35	0.591
Pseudoscleropodium purum		6.52 ± 0.05	$2.31 \cdot 10^{-6}$–$1.47 \cdot 10^{-3}$	1.15	$6 \cdot 10^{-3}$
				2.45	0.114
				6.20	40.266
Brachytecium rutabulum		6.62 ± 0.08	$3.11 \cdot 10^{-6}$–$1.23 \cdot 10^{-3}$	2.45	0.133
				4.60	1.329
				4.90	1.306
Hypnum sp.	Nickel	5.63 ± 0.03	$9.37 \cdot 10^{-6}$–$2.89 \cdot 10^{-3}$	1.25	0.073
Sphagnum sp.		5.65 ± 0.05	$9.88 \cdot 10^{-6}$–$3.17 \cdot 10^{-3}$	1.25	0.081
Pseudoscleropodium purum		5.67 ± 0.03	$9.08 \cdot 10^{-6}$–$2.41 \cdot 10^{-3}$	1.35	0.053
				5.70	7.669
Brachytecium rutabulum		5.58 ± 0.04	$9.37 \cdot 10^{-6}$–$2.91 \cdot 10^{-3}$	1.20	0.057
Hypnum sp.	Lead	6.55 ± 0.07	$1.93 \cdot 10^{-6}$–$9.93 \cdot 10^{-4}$	2.95	0.799
Sphagnum sp.		6.52 ± 0.05	$2.03 \cdot 10^{-6}$–$1.04 \cdot 10^{-3}$	2.05	0.137
				3.45	0.961
Pseudoscleropodium purum		6.55 ± 0.06	$1.98 \cdot 10^{-6}$–$1.03 \cdot 10^{-3}$	2.80	0.334
				6.00	50.400
Brachytecium rutabulum		6.53 ± 0.05	$2.03 \cdot 10^{-6}$–$6.97 \cdot 10^{-4}$	3.10	1.117
Hypnum sp.	Zinc	6.76 ± 0.05	$7.19 \cdot 10^{-6}$–$2.83 \cdot 10^{-3}$	2.15	0.084
				3.95	0.653
Sphagnum sp.		6.79 ± 0.08	$7.34 \cdot 10^{-6}$–$2.88 \cdot 10^{-3}$	2.05	0.059
				3.45	0.200
				6.10	28.601
Pseudoscleropodium purum		6.77 ± 0.05	$7.19 \cdot 10^{-6}$–$2.85 \cdot 10^{-3}$	2.25	0.095
				5.45	7.118
Brachytecium rutabulum		6.78 ± 0.06	$7.04 \cdot 10^{-6}$–$2.78 \cdot 10^{-3}$	2.40	0.116
				4.65	2.070

has a longer time to bind metals and increases the concentration of several metals inside the cells or cell walls [53]. Eventually, the difference in composition can also be explained by a different capacity to cation exchange, because of the differences in the chemical composition of the membranes and cell walls [54].

The concentrations of released metals during moss interaction with aqueous solution were significantly lower than those used in adsorption experiments. During the 9 h of solution exposure experiments, *Sphagnum* sp. and *Hypnum* sp. proved to be the most inert species in terms of both DOC and metal release, which is certainly linked to the specificity of their cell wall chemical composition as described below.

4.2. Acid–base properties of mosses

The amphoteric properties of the moss stem from acid–base dissociation of protonated organic moieties on the surface of the cell wall. The acid–base titration showed that *Sphagnum* sp. exhibits the highest excess of negative charges corresponding to its highest capacity for metal adsorption. The acid–base titration of 4 mosses demonstrated a certain variability of pK_a among mosses likely linked to the different compositions of their cell walls. In this study, *Hypnum* sp., *Sphagnum* sp., *P. purum* and *B. rutabulum* showed pK_a values ~4, 4.5–5.75, ~6–7.35, 8–9.15 and ~10. These pK_a can be tentatively related with carboxyl/phosphodiester, carboxyl, phosphoryl, amine and polyphenol functional groups. *Sphagnum* sp. contains the highest amount of total binding sites, followed by *P. purum* (15% smaller), *Hypnum* sp. (25% smaller) and *B. rutabulum* (25% smaller). It is important to note that *Sphagnum* sp. exhibits the dominance of carboxyl, phosphoryl, amine functional groups, the main metal-binding moieties on the biological surfaces [19,48]. As such, *Sphagnum* sp. is the most efficient metal adsorbent given the carboxyl and phosphoryl groups are the primary metal-binding groups at a high concentration of metals [55,56] whereas the sulphydryl and amine groups can be determinant especially under extreme pH conditions and low metal concentrations [57]. The pK_a computed reported for different microorganisms are around ~ 3, 4–5, 6–7 and 9–10 with total binding sites around 0.044–0.113 mmol g^{-1} of bacteria [39,48,57,58]. The relative percentage of functional groups for the different microorganisms inferred from surface titration (Fig. 6) showed that mosses possess a relatively higher percentage of carboxyl/phosphodiester, amine/polyphenol groups compared to bacteria [48,59] and cyanobacteria [43,60], whereas the number of carboxyl groups on mosses is smaller compared to bacteria.

Lignin and cellulose represent the main organic composition of the mosses cell walls [61]. These polysaccharides contain alcohols, aldehydes, ketones, acids, phenolic and hydroxides as the main functional groups. Accordingly, the carboxylic and phenolic groups have been suggested to be responsible for the adsorption of metals on peat moss [62], similar to humic and fulvic acids [63].

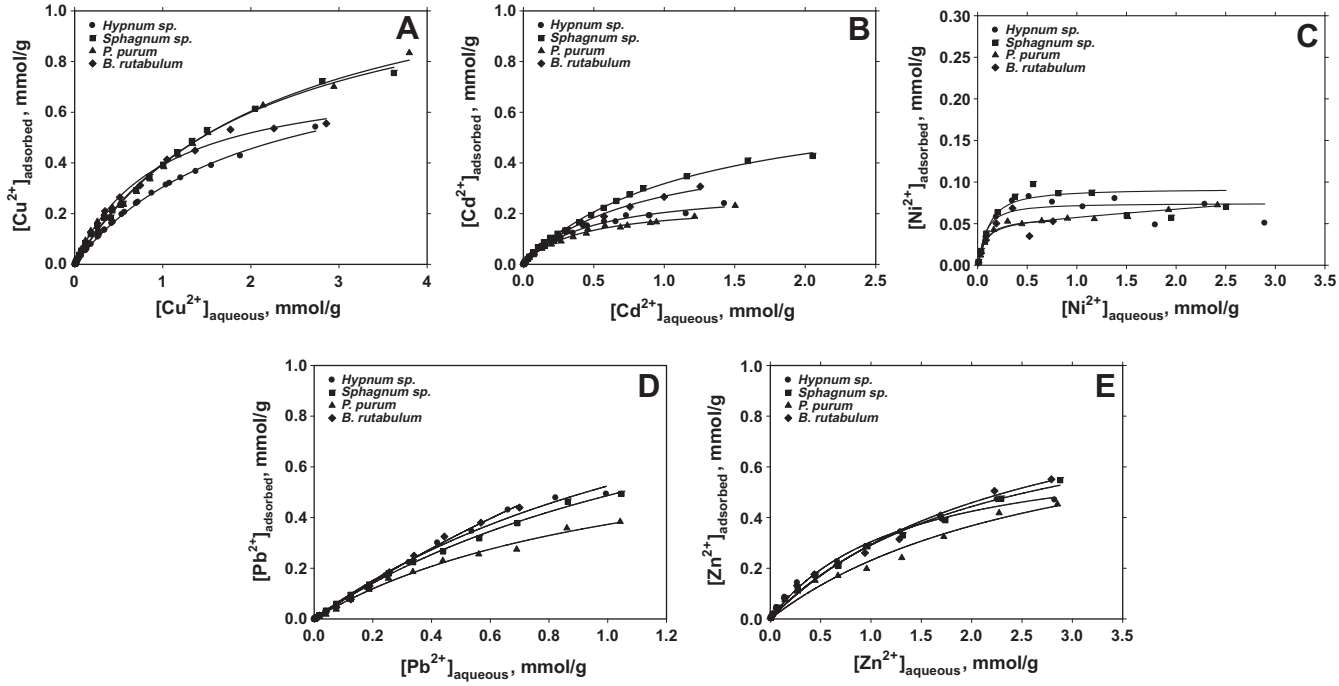

Fig. 5. Metal adsorbed onto moss surface as a function of metal concentration in solution (Langmurian-isotherm), in 0.01 M $NaNO_3$ and 1.0 $g_{dry}\ L^{-1}$ biomass at constant pH (see Table 3). Lines represent the LPM model results.

Table 4
Langmuir parameters computed from the experiments at different aqueous metal concentrations (Langmuirian isotherm).

Species	Metal studied	q_{max} mmol g^{-1}	K_L g $mmol^{-1}$
Hypnum sp.	Copper	0.994	0.437
Sphagnum sp.		1.288	0.443
Pseudoscleropodium purum		1.356	0.417
Brachytecium rutabulum		0.782	0.970
Hypnum sp.	Cadmiun	0.318	1.771
Sphagnum sp.		0.729	0.785
Pseudoscleropodium purum		0.263	2.047
Brachytecium rutabulum		0.456	1.385
Hypnum sp.	Nickel	0.089	9.155
Sphagnum sp.		0.107	7.081
Pseudoscleropodium purum		0.062	11.360
Brachytecium rutabulum		0.071	10.454
Hypnum sp.	Lead	1.509	0.531
Sphagnum sp.		1.109	0.746
Pseudoscleropodium purum		0.880	0.775
Brachytecium rutabulum		2.560	0.305
Hypnum sp.	Zinc	0.702	0.765
Sphagnum sp.		0.929	0.456
Pseudoscleropodium purum		0.901	0.344
Brachytecium rutabulum		1.049	0.388

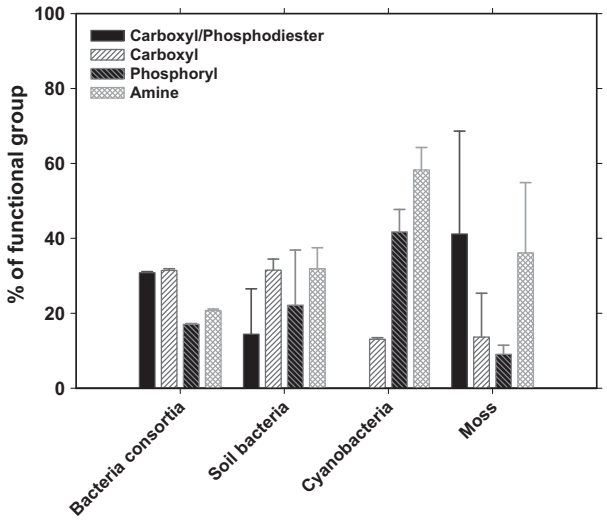

Fig. 6. Relative percentage of binding functional groups obtained from the acid–base titration for bacteria consortia [48], soil bacteria [39,59], cyanobacteria [43,60] and moss (this study).

4.3. Metal adsorption on mosses

All 4 studied mosses demonstrated very fast adsorption kinetics as the equilibrium or steady-state metal concentration in solution in contact with devitalized biomass is achieved within several minutes of reaction and remains constant over almost a month of exposure. This corroborated numerous previous observations on other biological surfaces on the fast equilibrium adsorption of divalent metals [64–66] and on organic-rich abiotic surfaces such as soils [67].

Heavy metals can be bound to most surface layers of cell wall through cation exchange, assimilated within the cells for cellular metabolism or distributed within the porous matrix of the surface layer. Regardless of the nature of final, biologically-active metal compartment in the cells, reversible adsorption on the cell surface represents the first and often limiting step of metal uptake by the microorganisms. Increasing the pH in solution leads to deprotonation of available surface sites that become therefore available to complex metals. The adsorption of metal on moss as a function of pH allowed us to rank the mosses according to their adsorption capacity for each metal. Considering the pH-edge adsorption, *B. rutabulum* seems to be the most efficient species because it reaches the highest percentage of adsorption and has the highest number of available sites for almost all the metals studied. However, high

DOC concentration released by *B. rutabulum* during its interaction with aqueous solution suggests its high instability in water and precludes its use as a biomonitor. In contrast, *Sphagnum* sp. seems to be the most promising species as a potential bioindicator, because it releases a relatively small amount of DOC and it is capable of efficiently binding metals in the full range of pH investigated as follows from its maximal adsorption capacity (q_{max}).

The number of major binding sites determined for mosses is equal to 34.8 mmol g^{-1} for Cu^{2+}, 40.3 mmol g^{-1} for Cd^{2+}, 7.7 mmol g^{-1} for Ni^{2+}, 50.4 mmol g^{-1} for Pb^{2+} and 28.6 mmol g^{-1} for Zn^{2+}. These values are significantly higher than those reported for other microorganisms which typically rank between 0.1 and 4 mmol g^{-1} of dry biomass, for aerobic soil bacteria *Pseudomonas aureofaciens* [39], heterotrophic bacteria [46,68], bacterial consortia [48], marine diatoms and freshwater species [69] and cyanobacteria [43].

The q_{max} obtained for 4 mosses was compared with that for aquatic plants [70–73], yeast [74], herbaceous peat [26,75], *Sphagnum* peat [26], fungus [20,76], bacteria [77,78], plants [79], algae [80,81] and soil [82]. The comparison is presented in Fig. 7. It can be clearly seen that the q_{max} value is the highest for mosses compared to all other studied organic surfaces, especially for Cu^{2+} and Pb^{2+} adsorption. Aquatic plants were the second group with highest adsorption capacities, reaching the maximum adsorption capacity in *P. luceus* with q_{max} = 0.496 mmol g^{-1} for Zn^{2+} and 0.642 mmol g^{-1} for Cu^{2+} [70]. Herbaceous peat also demonstrated significant adsorption capacities, although much lower than the mosses. Overall, the mosses examined in this study exhibit one of the highest adsorption capacity among all known biological sorbents and as such can be efficient candidates for the environmental biomonitoring application.

4.4. Universal adsorption parameters

The adsorption of metals on mosses as a function of pH follows a universal adsorption pattern that is well comparable with other organic materials. In Fig. 3 we presented a pH-dependent adsorption edge for bacteria consortia and individual bacteria species obtained at experimental conditions very similar to those used in the present study. In full accord with numerous previous observations [40,43,47,48,64,83], the existence of "universal metal (Cu^{2+}, Cd^{2+}, Ni^{2+}, Pb^{2+}, and Zn^{2+}) adsorption edge" both for bacteria and bryophyte can be concluded. In contrast to former studies, dealing only with Cd^{2+} for establishing this "universal edge", this study extends to 4 other important divalent metals, all of them with a similar universal dependence on the percentage of adsorption on pH. This finding should certainly facilitate quantitative modeling of metal interaction with biosorbents under various environmental conditions.

The universal adsorption edge, consisting in similarity of the pH-dependent adsorption edge on various biosorbents for each metal, likely stem from the dominance of carboxylates and phosphorylates as the main binding sites for metal complexation at the moss surface. The same binding sites are most frequently reported on bacteria [39,40,43,48,64], peryphytic biofilms [67] and diatoms [22]. Consequently, regardless of the biological nature of the sample and the bacteria/plankton/plant kingdom, the adsorption curve remains rather similar reflecting the dominance of main metal-binding moieties. However, given their (1) large surface area, (2) high stability of devitalized mosses in aqueous solution, notably *Sphagnum* sp., and (3) low cost of natural or artificially grown (notably cloned) moss species, devitalized moss should remain by far the best biomonitor that can be used for passive adsorption of divalent metals.

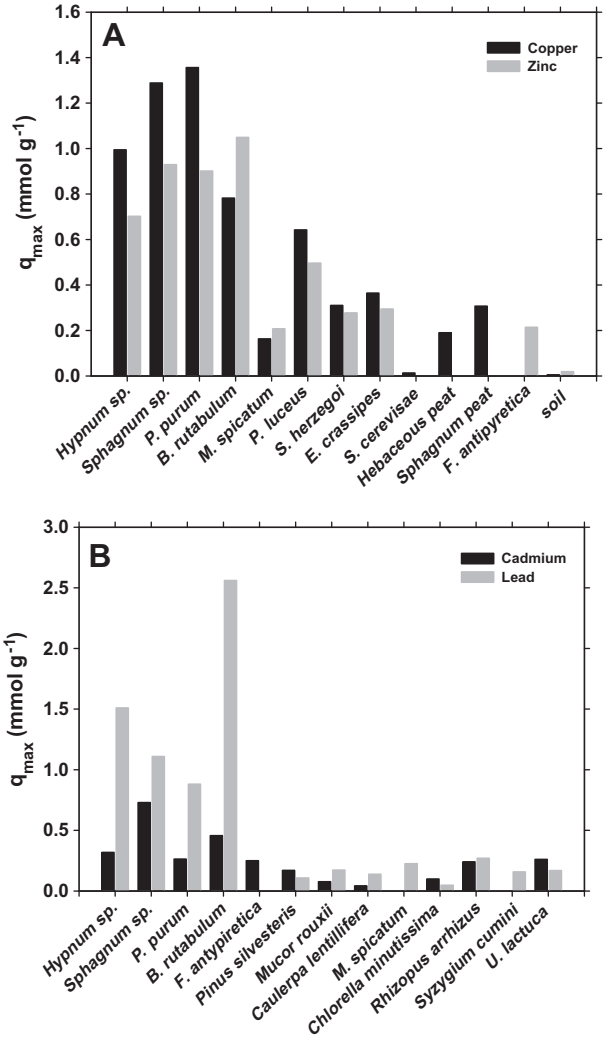

Fig. 7. The value of q_{max} for (A) copper and zinc and (B) cadmium and lead. These data were collected from the literature for aquatic plants [70–73], yeast [74], herbaceous peat [26,75], *Sphagnum* peat [26], fungus [20,76], bacteria [77,78], plants [79], algae [80,81] and soil [82].

5. Conclusions

The interaction of 5 heavy metals (Cu^{2+}, Cd^{2+}, Ni^{2+}, Pb^{2+} and Zn^{2+}) with 4 mosses (*Hypnum* sp., *Sphagnum* sp., *P. purum* and *B. rutabulum*) demonstrated their potential use as bioindicator of atmospheric pollution. Via combining thorough solid and solution analyses, including surface acid–base titration, pH-dependent adsorption edge and "Langmuirian" adsorption at constant pH and variable metal concentration, we conclude that *Sphagnum* sp. exhibits the highest proton and metal adsorption capacity while being most stable in aqueous solution in terms of DOC release and biomass degradation. Compared with other biosorbents, mosses possess significantly higher concentration of surface groups capable to bind divalent metals at the cell surface.

Acknowledgments

This study received financial support from the MOSSclone project by the European Union in the Seventh Framework Program (FP7) for Research and Technological Development. Additional support from the Russian Ministry of Science and Education and Tomsk State University (Mega-Grant BIO-GEO-CLIM No.

14.B25.31.0001) is also acknowledged. We also thank Katrin Meier for the English revision of the manuscript.

Appendix A. Supplementary material

Supplementary data associated with this article can be found, in the online version, at http://dx.doi.org/10.1016/j.jcis.2013.10.028.

References

[1] N. Bernard, M. Saintot, C. Astre, M. Gerber, Arch. Environ. Health: Int. J. 53 (2) (1998) 122–128.
[2] M. Saintot, N. Bernard, C. Astre, M. Gerber, Arch. Environ. Health: Int. J. 54 (1) (1999) 34–39.
[3] M. Saintot, N. Bernard, C. Astre, P. Galan, S. Hercberg, M. Gerber, Revue d'épidémiologie et de santé publique 48 (2000) 2S54.
[4] M.J. McLaughlin, D. Parker, J. Clarke, Field Crop. Res. 60 (1) (1999) 143–163.
[5] A. Brinkman, The Bryologist 32 (1929) 29–31.
[6] O. Gilbert, in: AirPollution-Proc.-1st Eur. Cong.- Influe Air Pollution Plants and Animals, Wageningen, 1969 (Ch. The effects of SO2 on lichens and bryophytes around Newcastle-upon-Tyne, pp. 223–235).
[7] B. Whitton, P. Say, J. Wehr, Use of plants to monitor heavy metals in rivers, in: Heavy Metals in Northern England: Environmental and Biological Aspects, Department of Botany, University of Durham, England, 1981, pp. 135–145.
[8] C. Mouvet, Environ. Technol. 5 (12) (1984) 541–548.
[9] C. Mouvet, Verh. Int. Ver. Limnol. 22 (4) (1985) 2420–2425.
[10] M. Kelly, C. Girton, B. Whitton, Water Res. 21 (11) (1987) 1429–1435.
[11] E.P. Gonçalves, R.A. Boaventura, C. Mouvet, Sci. Total Environ. 114 (1992) 7–24.
[12] E.P. Gonçalves, H.M. Soares, R.A. Boaventura, A.A. Machado, J.C. Esteves da Silva, Sci. Total Environ. 142 (3) (1994) 143–156.
[13] J.M. Glime, Flora North Am. 27 (2007) 14–41.
[14] J. Fabure, C. Meyer, F. Denayer, A. Gaudry, D. Gilbert, N. Bernard, Water Air Soil Pollut. 212 (1–4) (2010) 205–217.
[15] N. Abdel-Jabbar, S. Al-Asheh, B. Hader, Sep. Sci. Technol. 36 (13) (2001) 2811–2833.
[16] Y. Ho, D.J. Wase, C. Forster, Water Res. 29 (5) (1995) 1327–1332.
[17] S. Al-Asheh, Z. Duvnjak, Adv. Environ. Res. 2 (1997) 194–212.
[18] J.B. Fein, C.J. Daughney, N. Yee, T. Davis, Geochim. Cosmochim. Acta 61 (1997) 3319–3328.
[19] J.B. Fein, A.M. Martin, P.G. Wightman, Geochim. Cosmochim. Acta 65 (23) (2001) 4267–4273.
[20] E. Fourest, J.-C. Roux, Appl. Microbiol. Biotechnol. 37 (3) (1992) 399–403.
[21] M. Gonzalez-Davila, J.M. Santana-Casiano, J. Perez-Pena, F.J. Millero, Environ. Sci. Technol. 29 (2) (1995) 289–301.
[22] A. Gélabert, O. Pokrovsky, J. Schott, A. Boudou, A. Feurtet-Mazel, J. Mielczarski, E. Mielczarski, N. Mesmer-Dudons, O. Spalla, Geochim. Cosmochim. Acta 68 (20) (2004) 4039–4058.
[23] O. Pokrovsky, G. Pokrovski, L. Shirokova, A. Gonzalez, E. Emnova, A. Feurtet Mazel, Geobiology 10 (2012) 130–149.
[24] B. Goffinet, W. Buck, Mol. Syst. Bryophytes 98 (2004) 205–239.
[25] M. Hübers, H. Kerp, Geology 40 (8) (2012) 755–758.
[26] R. Gündogan, B. Acemioglu, M.H. Alma, J. Colloid Interface Sci. 269 (2) (2004) 303–309.
[27] E. Rojas, L.A. Herrera, L.A. Poirier, P. Ostrosky-Wegman, Mutat. Res./Genet. Toxicol. Environ. Mutagen. 443 (1–2) (1999) 157–181.
[28] F. Calevro, S. Campani, C. Filippi, R. Batistoni, P. Deri, S. Bucci, M. Ragghianti, G. Mancino, Aquat. Ecosyst. Health Manage. 2 (3) (1999) 281–288.
[29] J. Blasiak, J. Kowalik, Mutat. Res./Genet. Toxicol. Environ. Mutagen. 469 (1) (2000) 135–145.
[30] L. Amor, C. Kennes, M. Veiga, Bioresour. Technol. 78 (2) (2001) 181–185.
[31] S. Kawanishi, S. Inoue, S. Oikawa, N. Yamashita, S. Toyokuni, M. Kawanishi, K. Nishino, Free Radical Biol. Med. 31 (1) (2001) 108–116.
[32] S. Monni, C. Uhlig, E. Hansen, E. Magel, Environ. Pollut. 112 (2) (2001) 121–129.
[33] D. Strausak, J.F. Mercer, H.H. Dieter, W. Stremmel, G. Multhaup, Brain Res. Bull. 55 (2) (2001) 175–185.
[34] H. Lefcort, E. Ammann, S. Eiger, Arch. Environ. Contam. Toxicol. 38 (3) (2000) 311–316.
[35] F. De Nicola, F. Murena, M.A. Costagliola, A. Alfani, D. Baldantoni, M.V. Prati, L. Sessa, V. Spagnuolo, S. Giordano, Environ. Sci. Pollut. Res. 20 (7) (2013) 1–11.
[36] S. Giordano, P. Adamo, V. Spagnuolo, M. Tretiach, R. Bargagli, Chemosphere 90 (2) (2013) 292–299.
[37] P. Adamo, S. Giordano, S. Vingiani, R. Castaldo, Environ. Pollut. 122 (1) (2003) 91–103.
[38] P. Adamo, P. Crisafulli, S. Giordano, V. Minganti, P. Modenesi, F. Monaci, E. Pittao, M. Tretiach, R. Bargagli, Environ. Pollut. 146 (2) (2007) 392–399.
[39] A. González, L. Shirokova, O. Pokrovsky, E. Emnova, R. Martínez, J. Santana Casiano, M. González-Dávila, G. Pokrovski, J. Colloid Interface Sci. 350 (1) (2010) 305–314.
[40] O.S. Pokrovsky, R.E. Martinez, E.I. Kompantseva, L.S. Shirokova, Chem. Geol. 335 (2013) 75–86.
[41] J.D. Allison, D.S. Brown, J. Kevin, MINTEQA2/PRODEFA2, A Geochemical Assessment Model for Environmental Systems: Version 3.0 User's Manual, Environmental Research Laboratory, Office of Research and Development, US Environmental Protection Agency, Athens, Georgia, USA, 1991.
[42] A. Martell, R. Smith, R. Motekaitis, Critically selected stability constants of metal complexes database, NIST Standard Reference Database 46.
[43] O.S. Pokrovsky, R.E. Martinez, S.V. Golubev, E.I. Kompantseva, L.S. Shirokova, Appl. Geochem. 23 (9) (2008) 2574–2588.
[44] J.S. Cox, S. Smith, L.A. Warren, F.G. Ferris, Environ. Sci. Technol. 33 (1999) 4514–4521.
[45] I. Sokolov, D. Smith, G. Henderson, Y. Gorby, F. Ferris, Environ. Sci. Technol. 35 (2) (2001) 341–347.
[46] R.E. Martinez, D.S. Smith, E. Kulczycki, F.G. Ferris, J. Colloid Interface Sci. 253 (1) (2002) 130–139.
[47] N. Yee, J. Fein, Geochim. Cosmochim. Acta 65 (13) (2001) 2037–2042.
[48] D. Borrok, J.B. Fein, Geochim. Cosmochim. Acta 68 (2004) 3043–3052.
[49] J. Febrianto, A. Kosasih, J. Sunarso, J. Yi-Hsu, J. Hazard. Mater. 162 (2009) 616–645.
[50] R. Bargagli, E. Battisti, E. Cardaioli, P. Formichi, L. Nelli, Inquinamento 36 (2) (1994) 48–58.
[51] R. Bargagli, D. Brown, L. Nelli, Environ. Pollut. 89 (2) (1995) 169–175.
[52] M. Castello, Environ. Monit. Assess. 133 (1–3) (2007) 267–276.
[53] H. Zechmeister, J. Bryol. 18 (3) (1995) 455–468.
[54] D. Brown, Mineral nutrition, Bryophyte Ecology, Springer, 1982. pp. 383–444.
[55] M. Boyanov, S. Kelly, K. Kemner, B. Bunker, J. Fein, D. Fowle, Geochim. Cosmochim. Acta 67 (18) (2003) 3299–3311.
[56] O.S. Pokrovsky, G.S. Pokrovski, A. GÃclabert, J. Schott, A. Boudou, Environ. Sci. Technol. 39 (12) (2005) 4490–4498.
[57] B. Mishra, M. Boyanov, B.A. Bunker, S.D. Kelly, K.M. Kemner, J.B. Fein, Geochim. Cosmochim. Acta 74 (15) (2010) 4219–4233.
[58] J.B. Fein, J.-F. Boily, N. Yee, D. Gorman-Lewis, B.F. Turner, Geochim. Cosmochim. Acta 69 (5) (2005) 1123–1132.
[59] M. Ueshima, B.R. Ginn, E.A. Haack, J.E.S. Szymanowski, J.B. Fein, Geochim. Cosmochim. Acta 72 (24) (2008) 5885–5895.
[60] R.E. Martinez, O.S. Pokrovsky, J. Schott, E.H. Oelkers, J. Colloid Interface Sci. 323 (2) (2008) 317–325.
[61] B.S. Gupta, M. Curran, S. Hasan, T. Ghosh, J. Environ. Manage. 90 (2) (2009) 954–960.
[62] L. Ringqvist, I. Öborn, Water Res. 36 (9) (2002) 2233–2242.
[63] T. Karlsson, Complexation of cadmium, copper and methyl mercury to functional groups in natural organic matter, PhD Thesis, 2005.
[64] O.S. Pokrovsky, J. Viers, E.E. Emnova, E.I. Kompantseva, R. Freydier, Geochim. Cosmochim. Acta 72 (7) (2008) 1742–1757.
[65] A. Gélabert, O. Pokrovsky, J. Schott, A. Boudou, A. Feurtet-Mazel, Geochim. Cosmochim. Acta 71 (15) (2007) 3698–3716.
[66] J. Ha, A. Gélabert, A.M. Spormann, G.E. Brown Jr., Geochim. Cosmochim. Acta 74 (1) (2010) 1–15.
[67] O. Pokrovsky, A. Feurtet-Mazel, R. Martinez, S. Morin, M. Baudrimont, T. Duong, M. Coste, Appl. Geochem. 25 (3) (2010) 418–427.
[68] C. Lamelas, M. Benedetti, K.J. Wilkinson, V.I. Slaveykova, Chemosphere 1362 (2006) 1370.
[69] A. Gélabert, O. Pokrovsky, J. Viers, J. Schott, A. Boudou, A. Feurtet-Mazel, Geochim. Cosmochim. Acta 70 (4) (2006) 839–857.
[70] O. Keskinkan, M. Goksu, A. Yuceer, M. Basibuyuk, C. Forster, Process Biochem. 39 (2) (2003) 179–183.
[71] T. Wang, J. Weissman, G. Ramesh, R. Varadarajan, J. Benemann, Bull. Environ. Contam. Toxicol. 57 (5) (1996) 779–786.
[72] I.A.H. Schneider, J. Rubio, Environ. Sci. Technol. 33 (13) (1999) 2213–2217.
[73] P. Pavasant, R. Apiratikul, V. Sungkhum, P. Suthiparinyanont, S. Wattanachira, T.F. Marhaba, Bioresour. Technol. 97 (18) (2006) 2321–2329.
[74] A. Öztürk, T. Artan, A. Ayar, Colloids Surf., B 34 (2) (2004) 105–111.
[75] T. Gosset, J.-L. Trancart, D.R. Thévenot, Water Res. 20 (1) (1986) 21–26.
[76] G. Yan, T. Viraraghavan, Water Res. 37 (18) (2003) 4486–4496.
[77] A. Öztürk, J. Hazard. Mater. 147 (1) (2007) 518–523.
[78] R.J. Martins, R. Pardo, R.A. Boaventura, Water Res. 38 (3) (2004) 693–699.
[79] R. Rakhshaee, M. Khosravi, M.T. Ganji, J. Hazard. Mater. 134 (1) (2006) 120–129.
[80] D. Roy, P.N. Greenlaw, B.S. Shane, J. Environ. Sci. Health A 28 (1) (1993) 37–50.
[81] A. Sarı, M. Tuzen, J. Hazard. Mater. 152 (1) (2008) 302–308.
[82] O.S. Pokrovsky, A. Probst, E. Leviel, B.-H. Liao, J. Hazard. Mater. 199 (2012) 358–366.
[83] B.R. Ginn, J.B. Fein, Geochim. Cosmochim. Acta 72 (16) (2008) 3939–3948.